

Tropical forests and the global carbon cycle: impacts of atmospheric carbon dioxide, climate change and rate of deforestation

Wolfgang Cramer^{1,2*}, Alberte Bondeau¹, Sibyll Schaphoff¹, Wolfgang Lucht¹, Benjamin Smith³ and Stephen Sitch¹

¹Potsdam Institute for Climate Impact Research, Department of Global Change and Natural Systems, PO Box 60 12 03, D-14412 Potsdam, Germany

²Institute of Geocology, Potsdam University, PO Box 60 15 53, D-14415 Potsdam, Germany

³Department of Physical Geography and Ecosystems Analysis, University of Lund, Sölvegatan 12, S-22362 Lund, Sweden

The remaining carbon stocks in wet tropical forests are currently at risk because of anthropogenic deforestation, but also because of the possibility of release driven by climate change. To identify the relative roles of CO₂ increase, changing temperature and rainfall, and deforestation in the future, and the magnitude of their impact on atmospheric CO₂ concentrations, we have applied a dynamic global vegetation model, using multiple scenarios of tropical deforestation (extrapolated from two estimates of current rates) and multiple scenarios of changing climate (derived from four independent offline general circulation model simulations). Results show that deforestation will probably produce large losses of carbon, despite the uncertainty about the deforestation rates. Some climate models produce additional large fluxes due to increased drought stress caused by rising temperature and decreasing rainfall. One climate model, however, produces an additional carbon sink. Taken together, our estimates of additional carbon emissions during the twenty-first century, for all climate and deforestation scenarios, range from 101 to 367 Gt C, resulting in CO₂ concentration increases above background values between 29 and 129 p.p.m. An evaluation of the method indicates that better estimates of tropical carbon sources and sinks require improved assessments of current and future deforestation, and more consistent precipitation scenarios from climate models. Notwithstanding the uncertainties, continued tropical deforestation will most certainly play a very large role in the build-up of future greenhouse gas concentrations.

Keywords: tropical forests; land use change; climate change; carbon balance; carbon dioxide

1. INTRODUCTION

There is general agreement about the importance of tropical forests for the global carbon cycle and hence global climate, but recent published estimates differ significantly for the area affected by tropical deforestation, the resulting flux of carbon to the atmosphere and the feedbacks of this flux to the climate system (cf. table 1; Houghton 1999; Fearnside 2000; Malhi & Grace 2000; Achard *et al.* 2002; DeFries *et al.* 2002). For some future climate-change scenarios, it has been shown that tropical forests could generate an unprecedented source of carbon, even in the absence of additional anthropogenic deforestation (Cox *et al.* 2000; Cramer *et al.* 2001). Assessing the future conditions of the Earth system requires better quantification of the significance of both direct deforestation and climate-driven changes in biospheric carbon stocks, compared with background 'reference' conditions. The primary question is whether the problem of climate-driven

carbon loss could exceed the relative importance of anthropogenic deforestation during the coming decades. If such an additional source appeared, then similar fossil fuel emissions would lead to a faster atmospheric CO₂ increase than before.

Throughout the more recent assessments of the Intergovernmental Panel on Climatic Change (IPCC), estimates of a global anthropogenic deforestation flux¹ of *ca.* 1.6 Gt C yr⁻¹ have been considered realistic (Bolin *et al.* 2000; Prentice *et al.* 2001) for the past 10–20 years. A new analysis of the spatial extent of tropical forest cover from long-term satellite time-series (DeFries *et al.* 2002) challenges these estimates as unrealistically high, claiming only 0.6 Gt C yr⁻¹ to be more probable for the 1980s and 0.9 Gt C yr⁻¹ for the 1990s. Using different sensors and methods, Achard *et al.* (2002) found a value of similar magnitude (0.64 ± 0.21 Gt C yr⁻¹ for 1990–1997). These large differences are not easily explained. If confirmed, they imply a modification of the global carbon budget that has implications for other compartments that are estimated with uncertainty, particularly the postulated Northern Hemisphere extratropical sink.

The problem of estimating deforestation-related fluxes consists of several sub-problems that are each associated

* Author for correspondence (Wolfgang.Cramer@pik-potsdam.de).

One contribution of 17 to a Theme Issue 'Tropical forests and global atmospheric change'.

Table 1. Recent estimates of carbon loss from tropical forests to the atmosphere attributed to deforestation (gigatonnes of carbon per year).

region	Houghton (1999)	Fearnside (2000)	Malhi & Grace (2000)	DeFries <i>et al.</i> (2002)	Achard <i>et al.</i> (2002)
	1980–1990	1981–1990	1980–1995	1980s	1990–1997
America	0.55 ± 0.3	0.94	0.94	0.37	—
Africa	0.29 ± 0.2	0.42	0.36	0.10	—
Asia	1.08 ± 0.5	0.66	1.08	0.18	—
total	1.90 ± 0.6	2.00	2.40	0.65	0.64 ± 0.21

with their own problems and uncertainties. First, estimating forest *area* is affected by the definitions of ‘forest’ versus ‘non-forest’ area, which vary widely in terms of tree size and density (see Noble *et al.* (2000) for a discussion of different uses of the term ‘forest’ for different statistical purposes). Discrepancies between current total flux estimates are also explained by the technology that is used for estimation of the area covered by ‘nearly intact forest’, such as ground-based surveys, aerial photographs or satellite images (see DeFries *et al.* (2002) for a discussion of discrepancies between different methods). Further, all area estimates must deal with the question of whether the deforested area is left bare, or is converted to a vegetation type with different carbon density, or undergoes regrowth (Houghton 1999).

Once the area is estimated, then the density of carbon in the removed vegetation needs to be assessed (e.g. as biomass per unit area). But total biomass is known for only a few ecosystems in a few locations, owing to the high effort required for measurement of all compartments (particularly the below-ground pool). Natural forests are spatially heterogeneous, owing to environmental conditions, management or natural disturbance history, even in the absence of deforestation.

Finally, the resulting carbon flux, including its temporal evolution, is usually the target as a comparison between the balance of the ecosystem without human interference and the deforested landscape. Direct measurements of such fluxes only exist from few and always undisturbed sites, for campaigns up to a few years. Even the undisturbed sites are affected by year-to-year climate variation, by trends in climate such as the anthropogenic enhancement of the greenhouse effect and possibly by direct CO₂ ‘fertilization’. By contrast, inventory-based approaches reconstruct the net balance over the time between inventories (usually many years), but they allow only very indirect estimations of the causes behind temporal and spatial variability. Reconstructing the overall carbon balance by inversion of atmospheric CO₂ concentrations is only a limited possibility for the tropics, because of sparse station network and uncertainties in estimating net uptake in undisturbed forests.

Improvement of carbon budget estimates, both for the reference value for recent tropical deforestation and for the climate-change-driven flux, requires that the quantities mentioned above are better constrained than previously. To integrate sparse information from surveys, statistics and imagery, and to allow extrapolation of current trends into the future, a combination of process-based numerical

models and parameters delivered from experiments and observations can be used. Once successfully tested against independent reconstructions, such an approach allows the use of scenarios of future developments.

The future role of tropical forests in the global carbon cycle and the climate system is a function of future deforestation rates and the degree to which remaining forests will be sustainable or even increase their carbon stock. Deforestation rates are strongly influenced by economic development and international agreements about the protection of forest resources. Future productivity in untouched or sustainably managed forests is influenced by climate change. Both factors, socio-economic development and climate change, carry major uncertainties for the coming decades. For the assessment of adaptation and mitigation options in tropical forest regions, it is of interest to relate these different uncertainties to each other and rate their relative importance.

2. METHODS AND DATA

(a) *Design*

Our quantitative assessment of the tropical forest carbon balance uses a scenario approach, based on a dynamic (global) vegetation model, driven by data on climate (monthly temperature and precipitation), atmospheric CO₂, soil texture and deforestation. The model is based on a quantitative understanding of relevant processes and is therefore expected to generate results that broadly capture environmental gradients and temporal trends, as well as the nonlinear evolution of carbon stocks in response to perturbations. Biomass stock and carbon flux estimates from this model have been tested successfully against a wide range of observations in several biomes. For tropical forests, we present some additional tests using different methods. As a first step of the application, we compare carbon fluxes attributable to historic deforestation with those attributed to other causes. Then, in a factorial experiment, we compare different plausible rates of future deforestation and different scenarios of regional climate change against each other, using the total carbon balance between atmosphere and biosphere as a diagnostic variable.

Previous assessments of carbon fluxes due to tropical deforestation have used inventory-based statistical approaches, sometimes supplied with additional data from remote sensing or from eddy covariance measurements at selected sites. The application of a process-based numerical model is expected to improve on such work when it can be assumed that major processes exhibit important and known nonlinear features (such as the different rates of decline in above- and below-ground carbon pools after

Table 2. Parameter values for tropical PFTs in the LPJ model (from Sitch *et al.* 2003).

(W/H indicates woody or herbaceous stature; z_1 and z_2 are the fraction of fine roots in the upper and lower soil layers, respectively; g_{\min} is the minimum canopy conductance; a_{leaf} is the leaf longevity; f_{leaf} , f_{sapwood} , f_{root} are the leaf, sapwood and fine root turnover times, respectively, and S_{GDD} is the growing degree day requirement to grow full leaf coverage.)

PFT	W/H	z_1 (-)	z_2 (-)	g_{\min} (mm s^{-1})	a_{leaf} (year)	f_{leaf} (yr^{-1})	f_{sapwood} (yr^{-1})	f_{root} (yr^{-1})	S_{GDD} ($^{\circ}\text{C}$)
tropical broad-leaved evergreen	W	0.85	0.15	0.5	2.0	0.5	0.05	0.5	—
tropical broad-leaved raingreen	W	0.70	0.30	0.5	0.5	1.0	0.05	1.0	—
tropical herbaceous	H	0.90	0.10	0.5	1.0	1.0	—	0.5	100

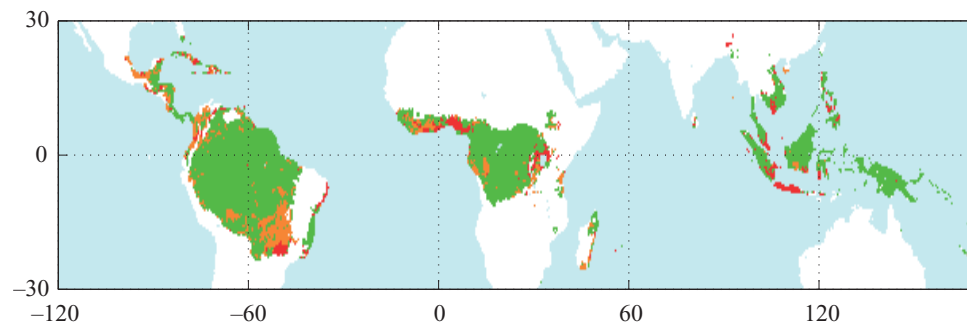


Figure 1. Global distribution of potential tropical forest area, simulated by the LPJ on the basis of 1980–1990 climate conditions (all colours) and of deforested areas according to the HYDE database (brown, marginal croplands; red, intensive croplands).

destruction of the canopy)—even when the parameters of these functions can be estimated from only a limited amount of empirical evidence. Such models typically allow for the study of feedbacks between changing atmospheric conditions and the fluxes of energy and matter through the biosphere.

(b) *The dynamic global vegetation model Lund–Potsdam–Jena*

DGVMs combine representations of biogeochemical processes with representations of processes contributing to the dynamics of vegetation structure and composition. Existing DGVMs (reviewed by Cramer *et al.* 2001) differ in their degree of complexity and suitability for different tasks. One common feature is their ‘generic’ formulation, which makes them suitable for broad-scale assessments in any biome. Typically, they use forcing data for climate and CO_2 concentration, thereby allowing the assessment of both direct and indirect (climatic) effects of CO_2 enrichment. The LPJ is a DGVM of intermediate complexity that has been shown to produce credible results for a range of applications (Sitch *et al.* 2003).

The LPJ includes, on the basis of 10 generalized PFTs, the major processes of vegetation dynamics, such as growth, competition and plant demography, as well as a mechanism for natural fire disturbance (Thonicke *et al.* 2001). For tropical ecosystems, the LPJ uses three different PFTs, named ‘tropical broad-leaved evergreen trees’, ‘tropical broad-leaved raingreen trees’ and ‘tropical herbaceous plants’. All three PFTs share the bioclimatic requirement that the mean temperature of the coldest month, calculated for 20 year running means, does not fall below 15.5°C (Prentice *et al.* 1992). The main parameters for the three PFTs are listed in table 2.

Inputs to the LPJ are monthly means of temperature, precipitation and cloudiness, as well as (static) soil texture and (annual) average atmospheric CO_2 concentration. From these, and based on available carbon pools and structural tissue from previous

years, the LPJ calculates daily GPP for each PFT on the basis of a widely used, mechanistic, coupled photosynthesis and water balance scheme (Farquhar *et al.* 1980; Haxeltine & Prentice 1996a,b; Sitch *et al.* 2003). In the LPJ implementation, the model incorporates simultaneous effects of temperature, moisture availability and ambient CO_2 concentration in a quasi-daily mode. From GPP, autotrophic (maintenance and growth) respiration is subtracted, as well as a cost for reproduction. Allometric relations are used annually to determine whether the remaining photosynthate is turned into long-lived or short-lived plant material, so creating different types of canopy architecture and litter quantities. Litter and soil organic matter decomposition are driven by seasonal temperatures and soil moisture status (calculated internally in the model). From this partitioning of GPP, the LPJ derives total fluxes such as NPP, heterotrophic respiration (R_h), emissions from natural fire disturbances² and, as a result, net ecosystem exchange. Because the water balance is tightly coupled to carbon fluxes, the model also yields actual evapotranspiration and local runoff. Comparison of total carbon stocks at different times gives NEP.

Of particular relevance for this study is the ability of LPJ to respond to the changing availability of water in a context where atmospheric CO_2 and temperature are also changing. Owing to the coupling of carbon and water balance, and the feedbacks between water availability and evapotranspiration, the model generally optimizes water use as real plants do, thereby adjusting leaf area and stomatal conductance to maintain the highest possible NPP. Despite these regulatory mechanisms, growth under water-stressed conditions includes an increased respiration cost, and NPP is reduced. Increased ambient CO_2 concentrations allow for reduced canopy conductance and therefore conserve water resulting in higher NPP. The magnitude of this effect, at the ecosystem level, over the longer term and in significantly higher-than-present ranges of CO_2 concentrations is currently poorly constrained by empirical or experimental observations.

Earlier studies seem to indicate, however, that the CO₂ response in the LPJ is over- rather than underestimated. For the climate-change response studied here, it follows that reduced water availability could possibly lead to even higher carbon releases than those presented below.

The LPJ has been tested successfully against a wide range of observations, including short-term flux measurements of carbon and water, satellite-based observations of leaf phenology and photosynthetic activity, inversions of atmospheric CO₂ measurements, and others (see, for example, Dargaville *et al.* 2002; Sitch *et al.* 2003). In a recent month-by-month analysis of vegetation activity in boreal forests for the period 1982–1998, the model generated vegetation dynamics with a high level of agreement with satellite observations, as well as with results from inversion studies of atmospheric CO₂ concentrations (Lucht *et al.* 2002). Comparisons between site-scale measurements of CO₂ exchange under ambient and enhanced CO₂ concentrations in the Duke Forest Free Air Carbon Dioxide Enrichment experiment with LPJ simulations also show a high level of confidence in the model's process formulations (T. Hickler, unpublished results).

The version of the LPJ presented here incorporates an improved representation of the water cycle compared with the model described by Sitch *et al.* (2003). The most important changes encompass the inclusion of additional processes such as interception and soil evaporation, and the daily distribution of precipitation. A few PFT parameters had to be readjusted to ensure realistic simulation of vegetation features and the carbon balance after the changes in the water-balance module. Similar to other DGVMs, the LPJ in this mode produces *potential natural vegetation*, i.e. the structure and carbon content of the biosphere in the absence of human impact.

To account for deforestation, we removed parts or all of the biomass in the affected grid cells, adding the loss to a total sum of all losses. The deforestation loss was estimated as follows: from a time-series of historical deforestation, we determined the amount of (additional) forest destruction in any given year and each grid cell. Based on the input data, the deforested area was turned into either 'intensive agriculture' or 'extensive agriculture'. The new carbon pools under extensive agriculture were estimated to correspond to a remaining 20% tree cover plus the carbon that would be stored in a natural grassland (the LPJ vegetation type that most closely resembles an agricultural cropping system). For intensive agriculture, all trees were removed and only grassland assumed to be the new condition. This simplistic approach to account for vegetation processes after deforestation was justified owing to the shortage of reliable data on area partitioning between different land-use types. It also represents the best estimation currently achievable, since insufficient parameter sets exist to account for process-based estimates of different land-use types.

(c) *Baseline data*

(i) *Climate and CO₂*

The LPJ requires data on climate and soils in the form of a grid and atmospheric CO₂. We used monthly fields of mean temperature, precipitation and cloud cover taken from the CRU05 (1901–1998) monthly climate data on a 0.5° × 0.5° global grid, provided by the CRU, University of East Anglia (New *et al.* 1999, 2000). Cloud cover data for 1997 and 1998, not so far compiled by CRU, were taken as the average over the previous 30 years. Monthly data were interpolated linearly to provide 'quasi-daily' time-series of climate. A dataset of historical global atmospheric CO₂ concentrations from 1901 to 1998 from various sources (ice-

core measurements and atmospheric observations), documented by Sitch *et al.* (2003) was used. Soil texture data were as in BIOME3 (Haxeltine & Prentice (1996a), based on the FAO soil dataset as in Zobler (1986) and FAO (1991)).

(ii) *Areas with potential and actual tropical forest*

Estimating the historical losses of carbon due to tropical deforestation requires an assessment of the area that may once have been occupied by tropical trees before large-scale land clearing, combined with a map of the present distribution. The area of potential distribution is, at the global level, well determined by climate (Prentice *et al.* 1992), but the present actual area is more difficult to assess. Data sources for the present distribution are regional and national forest inventories, aggregated by FAO to a global dataset (FAO 2003), and remote-sensing data from several platforms. Common to both data sources is that they depend on a consistent definition of 'forest' versus 'non-forest', usually requiring a more or less arbitrary cut-off value to be applied at the continuum between dense forest and open land. Remote sensing offers the advantage of greater consistency, shorter time-intervals between observations, although cloud cover and sub-pixel forest fragmentation present problems that are resolved only by approximate methods.

For this study, we have combined a long-term reconstruction of deforestation rates (HYDE, Klein Goldewijk 2001) with the potential forest area determined by the LPJ so as to achieve both a realistic estimate of current tropical forest cover and a framework which allows the application of deforestation scenarios for the future. Table 3 shows the resulting global total areas, contrasted against several alternative estimates. For all three world regions, the areas resulting from our approach are similar to those found by the most recent FAO assessment.

None of the other sources shows the area of potential distribution of tropical forests. It is therefore difficult to assess whether the resulting deforestation fluxes estimated by these studies result from different total reference areas (e.g. owing to different forest definitions) or from different measures of deforested area.

(iii) *Deforestation rates*

As an estimate of region-specific long-term historical deforestation rates, we used the HYDE dataset (Klein Goldewijk 2001), which provides land-cover classifications on a 0.5° × 0.5° longitude/latitude grid for the years 1700, 1750, 1800, 1850, 1900, 1950 and 1970.³ From HYDE, we assumed that deforestation had occurred on all grid cells classified as 'intensive agriculture' or 'extensive agriculture'. Between the time-slices, we interpolated deforestation linearly for each grid cell to provide a quasi-continuous yearly historical dataset. The resulting present-day tropical forest distribution is shown in figure 1.

(d) *Scenarios*

(i) *General considerations*

Because the future conditions of the Earth system depend on multiple interacting processes occurring within both the human society and the bio-physicochemical environment, none of the scenarios used in this study is intended to represent predictions of future conditions. Instead, they represent either conservative 'business as usual' assumptions (which may be unrealistic) or sets of multiple alternatives that can be traced back to simple assumptions.

Table 3. Tropical forest areas by continent, 1990 (10³ km²).

	Fearnside (2000)	Malhi & Grace (2000)	Achard <i>et al.</i> (2002)	FAO (2003)	this study
America	10238	8705	6690	9326	8070
Africa	5276	3730	1980	6369	3980
Asia	3106	2664	2830	4567	2740
total	18620	15099	11500	20261	14790

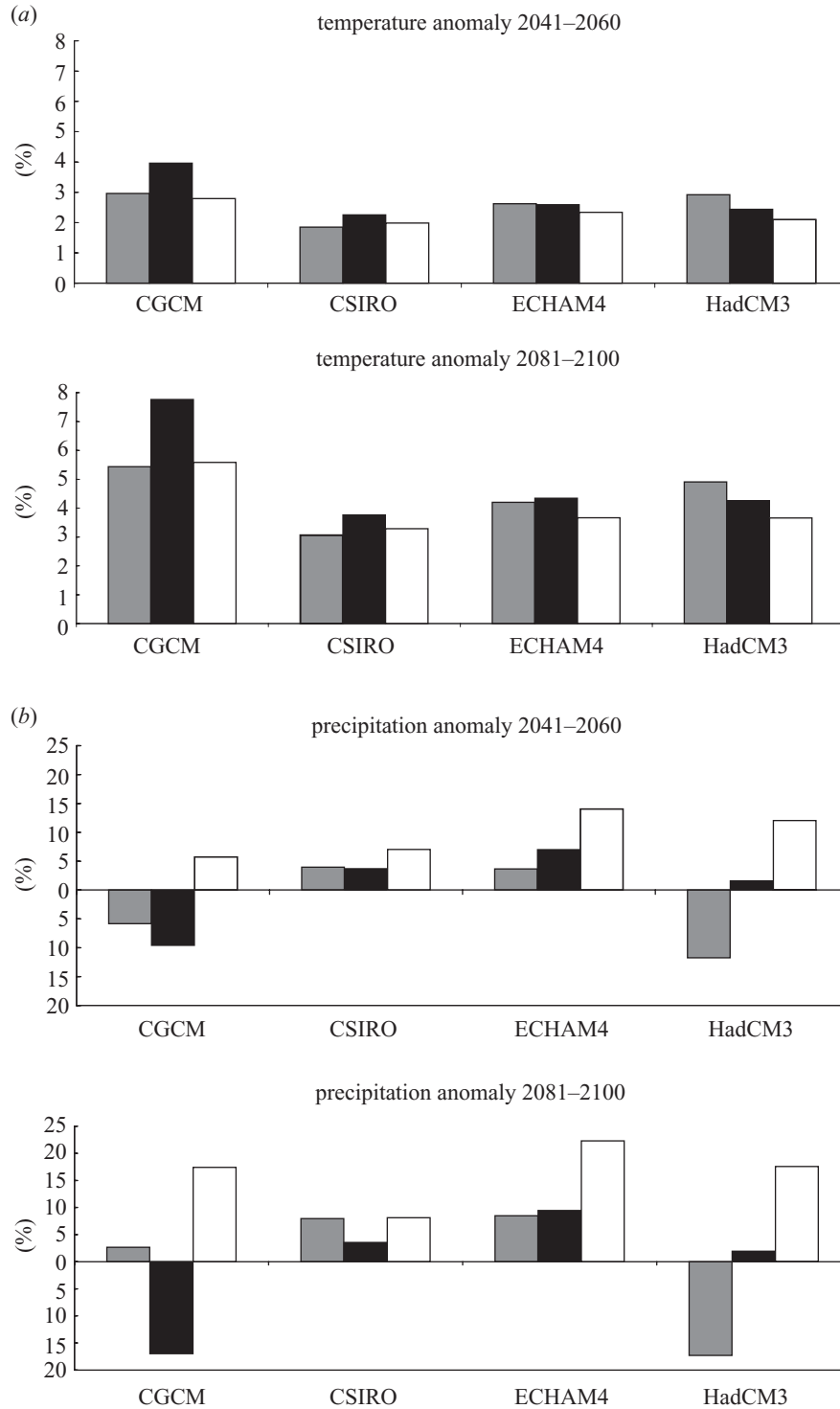


Figure 2. (a) Temperature anomalies for tropical regions (30° S – 30° N), for all four climate models, expressed as difference to the period 1969–1998. (b) Precipitation anomalies for tropical regions (30° S – 30° N), for all four climate models, expressed as difference to the period 1969–1998. (Grey bars, America; filled bars, Africa; open bars, Asia.)

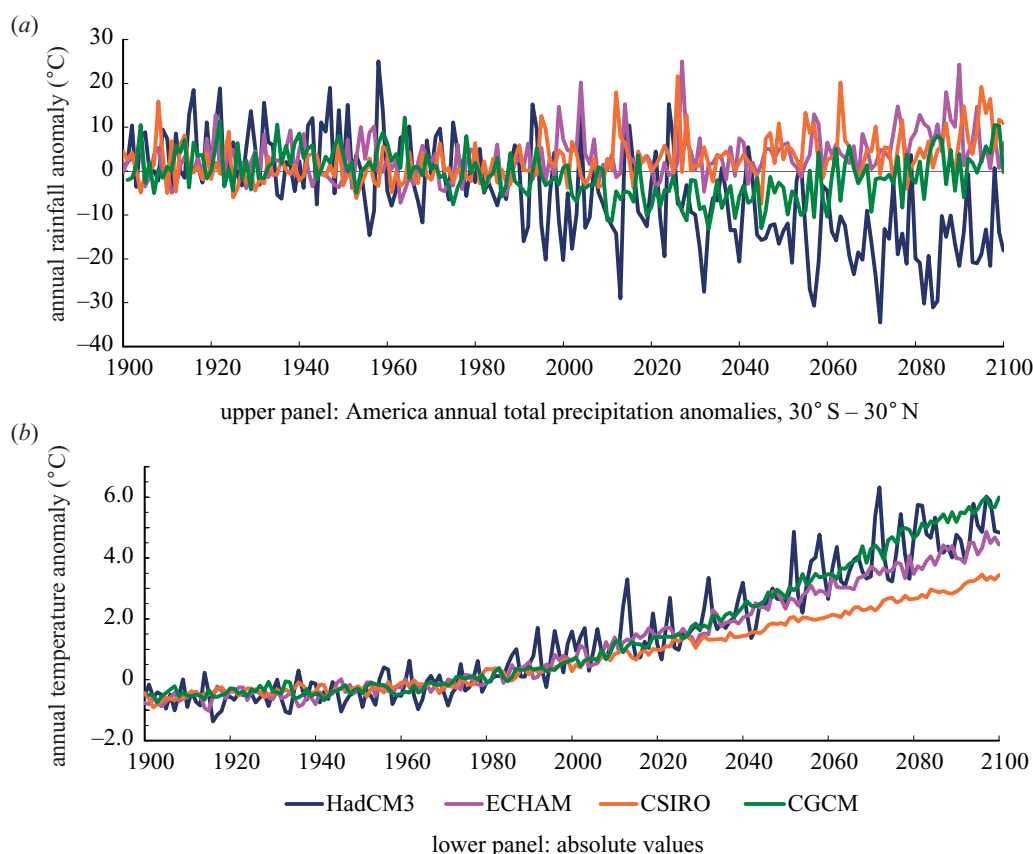


Figure 3. Climate reconstruction and scenario data for tropical America (30° S – 30° N) and the period 1901–2100, based on four different general circulation models. (a) Change in annual total rainfall (per cent) in relation to the average for 1969–1998. (b) Change in annual mean temperature in relation to the average for 1969–1998. Model simulations were made with monthly data.

Table 4. Forest areas, deforestation areas and remaining forest areas as used in this study. (The trend in future deforestation is used with a low and a high scenario, by direct extrapolation of trends reconstructed by Achard *et al.* (2002) ('low deforestation') and Malhi & Grace (2000) ('high deforestation').)

	forest area in 1900 (Klein Goldewijk 2001)		deforestation rates		remaining forest area in 2100			
			1990–1997 (Achard <i>et al.</i> 2002)	1990–1995 (Malhi & Grace 2000)	'low deforestation'		'high deforestation'	
	10 ⁷ km ²	potential area (%) ^a	10 ³ km ² yr ⁻¹	10 ³ km ² yr ⁻¹	10 ⁷ km ²	% of pot.	10 ⁷ km ²	% of pot.
America	9.66	94	22	56.9	4.92	48	2.07	20
Africa	4.39	89	7	37.0	2.15	44	0.65	13
Asia	3.24	93	20	35.1	0.43	12	0.02	< 1
total	17.28	92	49	129.0	7.49	40	2.74	15

^a As defined by the climatic limits in LPJ.

(ii) *Carbon dioxide*

For the period 1991–2100, all climate and DGVM simulations were based on the IPCC IS92a emission scenario (Houghton *et al.* 1992). This widely used scenario includes intermediate assumptions about human demography and economic activity, and causes an increase of CO₂ emissions into the atmosphere of ca. 1% yr⁻¹ CO₂ equiv. throughout the twenty-first century. For a long time, this scenario was considered a 'business as usual' scenario of carbon emissions and associated atmospheric CO₂ concentrations. Here, its use is mainly justified

owing to the fact that outputs are available for this scenario from several climate modelling centres, thereby allowing comparison between different climate models.

(iii) *Climate*

The climate-change scenarios are derived from output made by four different climate models, provided by the IPCC Data Distribution Center, covering the period 1901–2100. To generate climate information for future conditions, we first derived anomalies of monthly means (temperature, precipitation,

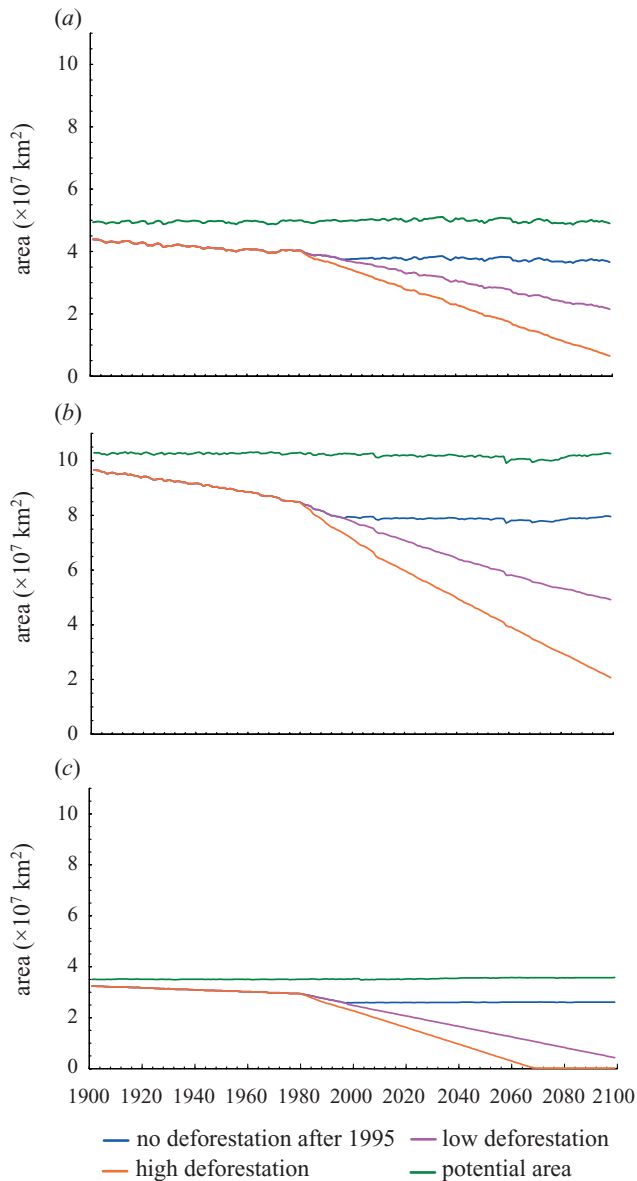


Figure 4. Forested areas with potential forest or influenced by the different deforestation scenarios (10^7 km^2). (a) Africa; (b) America; (c) Asia. Historical reconstructions follow HYDE (Klein Goldewijk 2001) until 1980 and Achard *et al.* (2002) ('low deforestation') or Malhi & Grace (2000) ('high deforestation'). Included also is a theoretical 'no deforestation after 1995' case. Interannual variability occurs owing to small changes in climatic potential from year to year.

cloudiness) from four different climate model outputs (CGCM1, CSIRO, ECHAM4, HadCM3)⁴ by calculating the differences between each modelled monthly value and a present-day baseline average for that month. These anomalies were then applied to a gridded baseline climate dataset (average 1969–1998 from the CRU dataset). This procedure retains the broad spatial features of climate change, as well as the monthly variability as simulated by the climate model, while ensuring that the spatial pattern and the general nature of present-day climate remain as in the observations. Interannual variability of the resulting time-series is driven by the climate model only. Therefore, no specific year in the calculations can be compared with a given true calendar year. To generate quasi-daily time-series of rainfall with appropriate statistical distribution we used the

30 year mean of 'wet days' from 1969 to 1998 of the CRU dataset and applied it to the whole time-series.

Indicative averaged anomalies of temperature and precipitation for these climate scenarios for tropical land areas are given in figure 2. During the twenty-first century, all scenarios show temperature increases on all continents, ranging from 1.9°C (CSIRO, America, 2041–2060) to 7.8°C (CGCM, Africa, 2081–2100). Scenarios differ considerably for precipitation. Although most models generate increased precipitation in tropical areas, magnitudes of the signal vary, and two models show notable exceptions: HadCM3 in America with a reduction of 17% by the end of the century and CGCM with a similar reduction in Africa.

Remarkably, climate scenarios not only differ in their broad spatial trends of precipitation, but also in their temporal variability in the tropical regions. Figure 3 illustrates this for the four climate models and the zone between 30°S and 30°N in America. The HadCM3 model clearly demonstrates much larger interannual variability than the other three models.

(iv) Deforestation

Scenarios of future deforestation were derived from two recent estimates of current trends. Based on the assessment of a variety of sources, Malhi & Grace (2000) conclude that, from 1990 to 1995, $129 \times 10^3 \text{ km}^2$ of tropical forests have been deforested each year. As one scenario, we extrapolate this value (differentiated for the three main areas America, Africa and Asia) linearly into the future. Directly based on a remote-sensing analysis covering a large sample of tropical forests, Achard *et al.* (2002) received much lower deforestation rates for the period 1990–1997: for total tropical forests $49.0 \times 10^3 \text{ km}^2 \text{ yr}^{-1}$. Extrapolation of these numbers yielded what is labelled 'low deforestation' (i.e. based on Achard *et al.* 2002) and 'high deforestation' (i.e. based on Malhi & Grace 2000), subsequently. The temporal evolution of the remaining forest areas is shown in figure 4. More detailed numbers are listed in table 4.

Deforestation scenarios were applied year by year, with uniform linear rates in each of the three regions, across all grid cells provided these carried any forest. For comparison, we also calculated scenarios with zero further deforestation after 1995. This way of allocating deforestation estimates is deliberately simplistic, because alternative methods would require many assumptions that could not be supported by data.

3. RESULTS

(a) Comparison of model results with other estimates of carbon pools and fluxes

To check the basic performance of the model in tropical forests, we report a comparison for biomass and productivity at typical sites in central Amazonia (near Manaus), and for the entire Amazon Basin. For these calculations, the LPJ was used with potential natural vegetation, run to equilibrium with pre-industrial climate, and then under the actual climate conditions reached at the end of the twentieth century, based on the CRU climate dataset. Malhi & Grace (2000) indicate a typical biomass stock for central Amazonian sites of 24.4 kg C m^{-2} . The LPJ simulates 22.5 kg C m^{-2} , using the observed climate of recent decades, which must be considered as a close agreement. The LPJ calculations for a similar grid cell with different climate in Malaysia (Borneo, at 114.5°E , 4°N) yield higher biomass values (35.2 kg C m^{-2}). This

is above the range of published values (12–29 kg C m⁻²) from four well-studied sites in Sarawak (Gunung, Mulu, Malaysia, 114.85° E, 4.08° N; Proctor 1999).

NPP has been found to vary widely throughout the Amazon. Malhi *et al.* (2004) report from several sites, based on stem increment measurements an average NPP of 663 g C m⁻² yr⁻¹, but they also list more productive sites in the western basin with more than 1000 g C m⁻² yr⁻¹. The corresponding LPJ result is 981 g C m⁻² yr⁻¹, an overestimation for the conditions at Manaus, but possibly nearer the average for the basin. Malhi *et al.* (2004) attribute within-basin productivity differences to soil fertility, which is not currently simulated in the LPJ. Direct measurements of heterotrophic respiration in similar stands and with comparable protocols are very difficult to find, and we were therefore unable to check the LPJ estimate of R_h of 931 g C m⁻² yr⁻¹. The resulting NEP of 50 g C m⁻² yr⁻¹ is confirmed indirectly by Phillips *et al.* (1998) who find a net biomass increase, averaged from several sites across the Amazon, of ca. 62 g C m⁻² a⁻¹ during recent decades.

Given the high uncertainty around site-based measurements in undisturbed forests, it appears difficult to close carbon budgets across a large area such as the entire Amazon Basin. Against the expectation of improved regional carbon balance estimates from atmospheric concentration measurements and inversion models, it is nevertheless justified to explore the potential of a modelling approach to calculate this balance. A study by Tian *et al.* (1998) estimated an average net sink for the Amazon of 0.22 Gt C yr⁻¹ for the period 1980–1990. Our calculations with the LPJ reach 50% of that value (0.11 Gt C yr⁻¹). Given that NEP is the difference between two very large fluxes (NPP and heterotrophic respiration), and that both fluxes are estimated with independent methods and parameterizations, this agreement must be considered fairly close. The climate-driven temporal variability (figure 5) of the LPJ balance is broadly similar to that estimated by Tian *et al.* (1998).

(b) *The response of tropical forests to changing CO₂, climate and deforestation*

At any location, ecosystems are simultaneously affected by radiation, temperature, moisture and nutrient availability, and direct interference such as anthropogenic deforestation. To illustrate the capacity of the model to adequately reflect these multiple forcings, we compare calculations for the Manaus site in two contrasting climate simulations (figure 6).

The left column of the diagram shows that, in the ECHAM4 simulation, the LPJ exhibits moderate interannual variability in productivity as well as soil respiration, reflecting slight changes in water availability owing to precipitation changes. In the twenty-first century, temperature increase leads to slightly accentuated drought stress, but interannual variability hardly changes. Productivity and respiration effects of increased drought are moderated by the direct effect of CO₂ increase (not shown; cf. Cramer *et al.* 2001; Sitch *et al.* 2003). The remaining drought stress reduces NPP slightly after about 2030 and yields increased mortality rates. Vegetation carbon pools

are somewhat reduced, but the litter and soil carbon pools do not increase, since the additional litter fall is immediately consumed by soil respiration. Around the model year 2042, the slight continuous change in temperature and precipitation appear to pass some threshold, giving a more marked increase in drought stress—this is followed by a reduction in vegetation carbon, which is not recovered during the remainder of the century.

Similar simulations with the HadCM3 model indicate differences already for the present day. Small differences in GPP and NPP, probably mostly because of lower moisture stress, produce a forest with significantly more live biomass. This climatic difference is caused by the technique we used for climate data production. For consistency, monthly anomalies from the climate model were applied throughout the time-series from 1900 to 2100. This results in identical long-term means for the period 1969–1998, but the interannual variability is determined by the climate model alone emerging as quite different between the two climate models. The comparison between ECHAM4 and HadCM3 for the model period 1969–1998 therefore illustrates that tropical forests in the LPJ are significantly affected by climate variability.

Climate simulated by HadCM3 in the twenty-first century undergoes dramatic changes in the American tropics. Although temperature increases at a rate similar to that of the ECHAM model, precipitation is reduced significantly, yielding a dramatic increase in drought stress. In addition, interannual variability increases strongly. Productivity and respiration respond to this variability in a synchronized way, i.e. the reduced litter fall in low productive years generates reduced soil respiration, despite the high temperatures. It therefore appears as if it is mostly the reduction in GPP that causes the large losses in vegetation carbon, which occur in the peak years of drought stress—and these losses are hardly recovered at all in more favourable years. The series of model years 2070–2072, with significantly higher temperatures and lower rainfall than before, then lead to a total collapse of vegetation at this site, with some increase in soil carbon and a very weak recovery towards the end of the century. In the model simulations, the loss of biomass appears to be a function of both dramatically increased climate variability and the increase in drought stress brought about by temperature increase as well as precipitation decline. Some shifts in PFT composition (favouring the more drought-adapted seasonal tropical trees) occur in response to climatic change and are already embedded in the quantities shown in the diagram.

Neither timing nor magnitude of climate fluctuations, as simulated by the climate models in this particular grid cell, may be taken as reliable forecasts of future environmental conditions at Manaus. However, they may serve as illustrations for the changing nature of the overall climatic regime that can be anticipated if greenhouse gas forcings and the process formulations in the models are formulated according to best current knowledge. The response of the ecosystem model to these fluctuations represents an extrapolation beyond experimentally proven model behaviour, but it is founded on the formulation of physiological processes that are checked against experimental evidence. As a conclusion, the probability of a vegetation collapse in the central Amazon cannot be determined with high

Table 5. Model-based estimates of carbon loss from tropical forests to the atmosphere attributed to deforestation.

	annual flux 1980–1995 (gigatonnes of carbon per year)			total flux 1901–1998 (gigatonnes of carbon)		
	Houghton (1999) ^a	this study		Houghton (1999) ^b	this study	
		low deforestation ^c	high deforestation ^d		low deforestation	high deforestation
America	0.55	0.40	0.70	30.5	18.61	24.38
Africa	0.29	0.18	0.32	9.5	8.99	11.21
Asia	1.08	0.30	0.49	38.6	11.06	13.83
total	1.90	0.89	1.51	79.0	38.65	49.36

^a Flux estimate averaged for 1980–1990.

^b Total for 1850–1990.

^c Deforestation rate for Achard *et al.* (2002).

^d Deforestation rate for Malhi & Grace (2000).

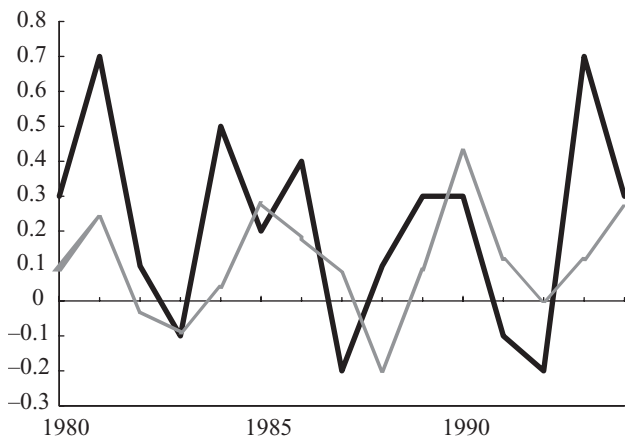


Figure 5. Interannual variability of sources and sinks in the Amazon Basin, between 1980 and 1998, estimated by the Terrestrial Ecosystem Model (Tian *et al.* 1998) and the LPJ.

accuracy; rather, these results must be seen as an illustration of the general rate and magnitude of response that tropical ecosystems could show if the physical environment changed as prescribed by the scenarios. Present-day analogues to such dry climates exist on the fringes of the central American tropical rainforest, and the LPJ simulations are also broadly in agreement with ecosystem conditions there.

(c) The carbon balance of global tropical forests

(i) Carbon fluxes due to past tropical deforestation

Table 5 summarizes our estimates of recent annual tropical carbon losses, as well as the total carbon loss to the atmosphere, caused by the combination of deforestation and climate change as it occurred during the twentieth century, and compares them with the extrapolations made by Houghton (1999). The LPJ estimates are separated by the 'low' (Achard *et al.* 2002) and 'high' (Malhi & Grace 2000) deforestation estimates for the most recent period, but are identical for the time until 1990 where the HYDE data were used. The main difference concerns Asian forests, which are estimated to produce much larger

fluxes by Houghton. For Africa and America, the book-keeping model and the LPJ with high deforestation rates yield broadly comparable numbers. The low deforestation case consequently gives lower flux estimates.

Table 5 also shows that the uncertainty about the actually deforested area (i.e. the difference between 'low' and 'high' deforestation) is rather large for the recent period. The comparison between recent fluxes and the century total demonstrates that this uncertainty also carries over to the total amounts.

(ii) Carbon fluxes due to tropical deforestation in the twenty-first century

Extrapolation of high and low deforestation trends into the twenty-first century, assuming changing atmospheric CO₂ according to IPCC IS92a, and changing climate as simulated by the four different climate models, yields widely differing carbon balances for each of the eight resulting scenarios, as well as for the case of 'no deforestation' (figure 7). Reflecting the reconstructions, the difference between deforestation scenarios is comparatively low in Asia (17–21%) and much higher in the Americas (26–105%) and Africa (50–117%).

In the 'no deforestation' scenario calculated with the CSIRO model, CO₂ increase and climate change generate a much more productive tropical forest zone, sequestering ca. 50 Gt of additional carbon. This is due to the much lower temperature increase simulated for America, combined with constantly wet conditions, both of which distinguish the CSIRO model from the other climate simulations (figure 3). By contrast, HadCM3 and CGCM1 show carbon sources solely due to climate change from some tropical forests, whereas ECHAM4 produces no significant sinks or sources. HadCM3 and CGCM1 differ strongly from each other: whereas HadCM3 locates the climate-driven source exclusively in the Americas (and generates sinks in both Africa and Asia), the source in CGCM1 is mostly in Africa and significantly also in the Americas. ECHAM4 and CSIRO distinguish much less between continents.

The climate-driven sink in the CSIRO calculation is greatly affected by the remaining forest area at each point

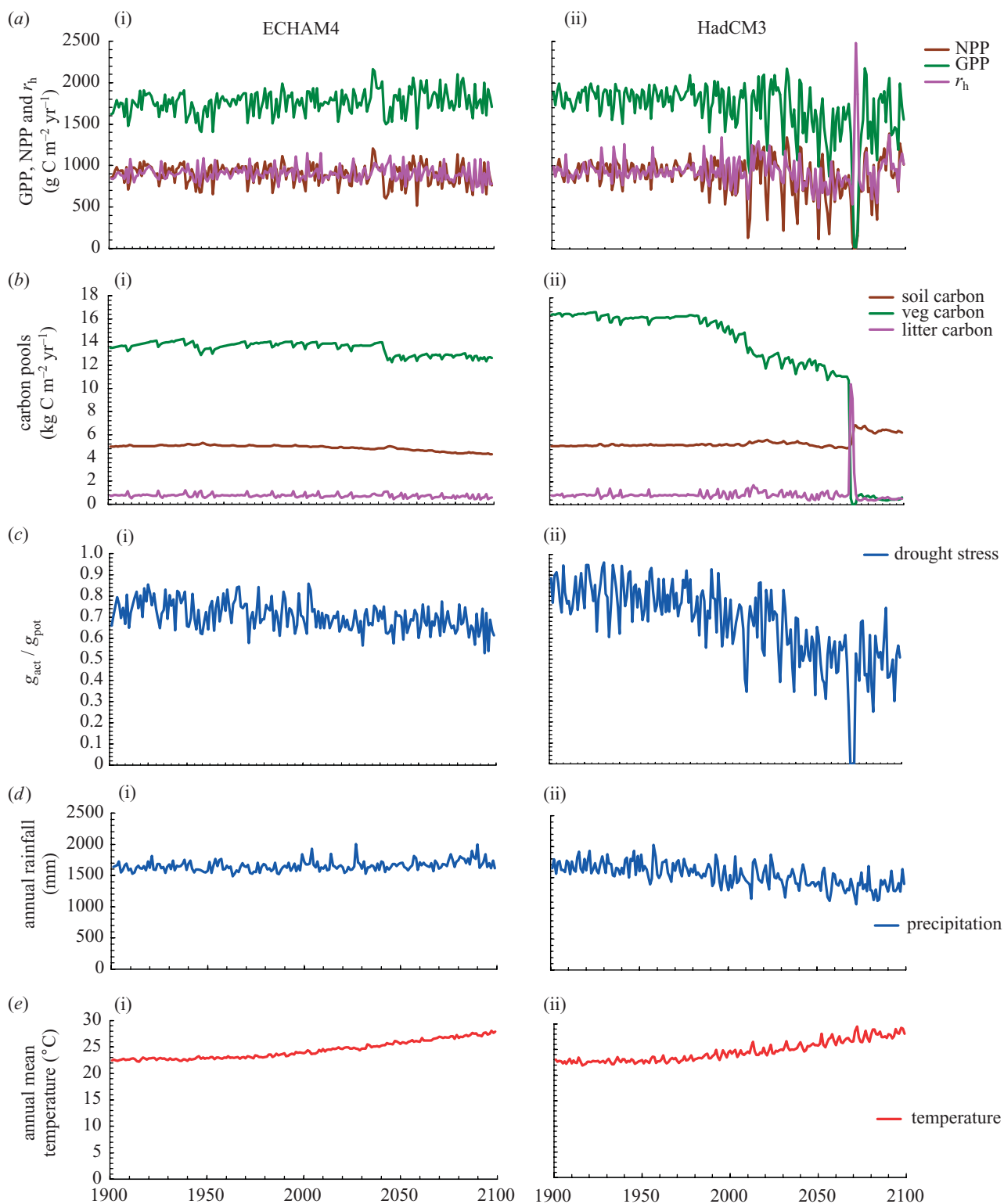


Figure 6. Carbon fluxes, pools and environmental factors in LPJ simulations for the Manaus site driven by output from two climate models: (i) ECHAM4 and (ii) HadCM3, without deforestation. (a) GPP, NPP and heterotrophic respiration (r_h) (grams of carbon per square metre per year); (b) soil, vegetation and litter carbon pools (kilograms of carbon per square metre) (vegetation carbon contains all structural biomass, above and below ground); (c) ratio between potential (unstressed) and actual canopy conductance, indicating the drought stress simulated by the LPJ (high values indicate low drought stress); (d) annual rainfall (mm); (e) annual mean temperature ($^{\circ}\text{C}$).

in time, and the simulation therefore shows the largest difference between no deforestation, low deforestation and high deforestation. For all models, the largest ‘high deforestation’ flux comes from America.

4. DISCUSSION

Overall, our comparison shows that the magnitude of anthropogenic deforestation still determines the larger

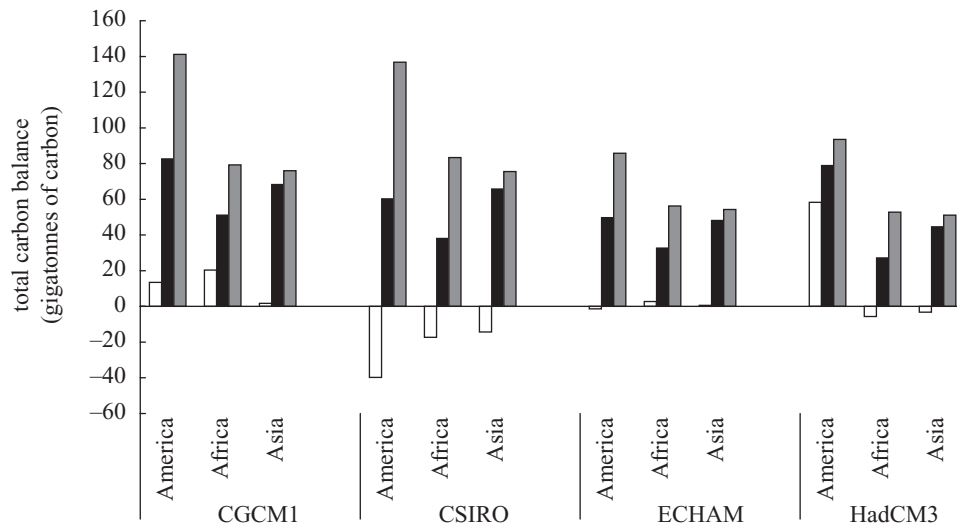


Figure 7. Total carbon balances (gigatonnes of carbon) for the twenty-first century, four different climate scenarios and three tropical forest regions, with no deforestation, low deforestation (Achard *et al.* 2002) and high deforestation rates (Malhi & Grace 2000), estimated by the LPJ, including effects of increased atmospheric CO₂ and climate on ecosystem processes. (Open bars, no deforestation; filled bars, low deforestation; grey bars, high deforestation.)

Table 6. Total twenty-first century carbon loss from tropical forests, for different climate and deforestation scenarios, calculated as the difference between the net balance of forests in the absence of deforestation and the scenario value (gigatonnes of carbon).

	low deforestation	high deforestation
CGCM1	-166.6	-261.0
CSIRO	-235.5	-367.1
ECHAM4	-128.5	-194.3
HadCM3	-101.3	-148.1

component of the role tropical forests will probably play in the global carbon cycle. The sources or sinks produced by climate change are significant components, however, and they strongly affect the spatial pattern of associated ecosystem changes.

Present rates of tropical forest destruction, even if they are confirmed to be at the low end of recent reconstructions, remain an important cause for concern, not only because of the negative impact the deforestation has on the environment of tropical regions, but also because of the amount of additional climate change that may be caused by the continuing release of carbon. In the most optimistic case, this carbon flux (if calculated as the difference between 'low deforestation' and 'no deforestation') still amounts to *ca.* 100 Gt C in the course of the twenty-first century (HadCM3)—the most pessimistic case ('high' minus 'no' deforestation) gives more than 360 Gt C (CSIRO) (table 6). Following the accounting scheme proposed by House *et al.* (2002), this range could lead to additional atmospheric CO₂ concentrations of between 29 and 129 p.p.m.

Further, the comparisons illustrate that the current uncertainty about global precipitation patterns as projected by climate models has great implications for the tropical forest zone and hence on feedbacks between climate change and the global carbon balance. More detailed analysis of the regional behaviour of climate models

should reveal whether the large Amazon dieback as shown by some of the models is indeed likely to occur in the coming decades.

A considerable uncertainty in the assessment remains with the natural carbon balance and also the disturbance regime of these forests. The discrepancy between recent productivity estimates in tropical forests, pointed out by Malhi & Grace (2000) and others, however, seems unlikely to greatly modify the broad-scale picture. If the much higher than believed net productivity estimates turn out to be realistic, then there must be an additional, previously unaccounted, flux in the root zone somewhere, as inferred by Richey *et al.* (2002), which either releases more carbon than assumed back into the atmosphere from the slow moving waters in flooded forests, or adds to the dissolved organic carbon flow in the major rivers. Because it is unlikely that this carbon remains on site, without being discovered, one may safely assume that the fluxes simulated by the LPJ have a realistic magnitude.

The uncertainty of flux estimates due to natural disturbances, however, is more problematic. We currently know far too little about the relation between deforestation activities and the natural disturbance regime, although several authors (e.g. Uhl & Kauffman 1990; Cochrane & Schulze 1998) have pointed out that undisturbed forests also burn more frequently once the landscape becomes more fragmented. Beyond fire, even less seems to be known about other natural disturbances in lowland forests, such as windstorms or insect outbreaks. There are too few observations and experimental evidence (despite Kauffman *et al.* (1988) and Uhl *et al.* (1988)) to support statistical or process-based models of these disturbances at present. Later versions of our model will also need realistic disturbance formulations for the tropical forest, and these may still change the overall balance to some extent.

The CRU05 climate data were kindly supplied by the Climate Impacts LINK Project (UK Department of the Environment Project EPG 1/1/16) on behalf of the Climatic Research Unit, University of East Anglia, UK. Comments and useful material for this paper were provided by Franz-W. Badeck, Potsdam

Institute for Climate Impact Research (PIK) and Kirsten Thonicke, Max-Planck Institute for Biogeochemistry, Jena, Germany. The authors also acknowledge the discussions with Yadvinder Malhi, Oliver Phillips and Jon Lloyd during the development of the final version of the manuscript.

ENDNOTES

¹Throughout this paper, carbon fluxes from the biosphere into the atmosphere ('sources') are given as positive numbers, and sinks as negative numbers, except for the case of local plant productivity estimates which are also given as positive numbers.

²The fire estimation algorithm in LPJ had been shown earlier to yield credible results in most biomes and to improve the overall carbon balance estimates (Thonicke *et al.* 2001). In the work leading to this study, however, it was found to significantly overestimate fire frequency and fire impacts for wet tropical forests. The disturbance scheme was therefore switched 'off' for the present analysis.

³The HYDE dataset provides numbers for 1990 as well, but for consistency with the scenario calculations, we used the values from Achard *et al.* (2002) and Malhi & Grace (2000) for this purpose.

⁴CGCM1: first version of the Canadian Global Coupled Model; CSIRO: Commonwealth Scientific and Industrial Research Organization global coupled ocean-atmosphere-sea-ice model; ECHAM4: ECMWF/HAMBURG model v. 4; HadCM3: Coupled atmosphere-ocean GCM developed at the Hadley Centre, Bracknell, UK; further details to be found at http://ipcc-ddc.cru.uea.ac.uk/dkrz/dkrz_index.html.

REFERENCES

- Achard, F., Eva, H. D., Stibig, H.-J., Mayaux, P., Gallego, J., Richards, T. & Malingreau, J.-P. 2002 Determination of deforestation rates of the world's humid tropical forests. *Science* **297**, 999–1002.
- Bolin, B., Sukumar, R., Ciais, P., Cramer, W., Jarvis, P., Kheshgi, H., Nobre, C., Semenov, S. & Steffen, W. 2000 *IPCC special report on land use, land-use change and forestry*, chapter 1. Cambridge University Press.
- Cochrane, M. A. & Schulze, M. D. 1998 Forest fires in the Brazilian Amazon. *Conserv. Biol.* **12**, 948–950.
- Cox, P. M., Betts, R. A., Jones, C. D., Spall, S. A. & Totterdell, I. J. 2000 Acceleration of global warming due to carbon-cycle feedbacks in a coupled climate model. *Nature* **408**, 184–187.
- Cramer, W. (and 16 others) 2001 Global response of terrestrial ecosystem structure and function to CO₂ and climate change: results from six dynamic global vegetation models. *Global Change Biol.* **7**, 357–373.
- Dargaville, R. J. (and 18 others) 2002 Evaluation of terrestrial carbon cycle models with atmospheric CO₂ measurements: results from transient simulations considering increasing CO₂, climate, and land-use effects. *Global Biogeochem. Cycles* **16**, 1092. (DOI 10.1029/2001GB001426.)
- DeFries, R. S., Houghton, R. A., Hansen, M. C., Field, C. B., Skole, D. & Townshend, J. 2002 Carbon emissions from tropical deforestation and regrowth based on satellite observations for the 1980s and 1990s. *Proc. Natl Acad. Sci. USA* **99**, 14 256–14 261.
- FAO 1991 The digitized soil map of the world (release 1.0). Technical report 67/1, Food and Agriculture Organization of the United Nations.
- FAO 2003 State of the world's forests. Technical report, United Nations Food and Agriculture Organization at <http://www.fao.org/DOCREP/005/Y7581E/Y7581E00.HTM>.
- Farquhar, G. D., von Caemmerer, S. & Berry, J. A. 1980 A biochemical model of photosynthetic CO₂ assimilation in leaves of C₃ plants. *Planta* **149**, 78–90.
- Fearnside, P. M. 2000 Global warming and tropical land-use change: greenhouse gas emissions from biomass burning, decomposition and soils in forest conversion, shifting cultivation and secondary vegetation. *Climat. Change* **46**, 115–158.
- Haxeltine, A. & Prentice, I. C. 1996a BIOME3: an equilibrium terrestrial biosphere model based on ecophysiological constraints, resource availability, and competition among plant functional types. *Global Biogeochem. Cycles* **10**, 693–709.
- Haxeltine, A. & Prentice, I. C. 1996b A general model for the light-use efficiency of primary production. *Funct. Ecol.* **10**, 551–561.
- Houghton, J. T., Callander, B. A. & Varney, S. K. (eds) 1992 *Climate change 1992: the supplementary report to the IPCC scientific assessment*. Cambridge University Press.
- Houghton, R. A. 1999 The annual net flux of carbon to the atmosphere from changes in land use 1850–1990. *Tellus B* **51**, 298–313.
- House, J. I., Prentice, I. C. & Le Quéré, C. 2002 Maximum impacts of future reforestation or deforestation on atmospheric CO₂. *Global Change Biol.* **8**, 1047–1052.
- Kauffman, J. B., Uhl, C. & Cummings, D. L. 1988 Fire in the Venezuelan Amazon 1: fuel biomass and fire chemistry in the evergreen rainforest of Venezuela. *Oikos* **53**, 167–175.
- Klein Goldewijk, K. 2001 Estimating global land use change over the past 300 years: the HYDE database. *Global Biogeochem. Cycles* **15**, 417–434.
- Lucht, W., Prentice, I. C., Myneni, R. B., Sitch, S., Friedlingstein, P., Cramer, W., Bousquet, P., Buermann, W. & Smith, B. 2002 Climatic control of the high-latitude vegetation greening trend and Pinatubo effect. *Science* **296**, 1687–1689.
- Malhi, Y. & Grace, J. 2000 Tropical forests and atmospheric carbon dioxide. *Trends Ecol. Evol.* **15**, 332–337.
- Malhi, Y. (and 27 others) 2004 The above-ground wood productivity and net primary productivity of 104 neotropical forest plots. *Global Change Biol.* **10**. (In the press.)
- New, M., Hulme, M. & Jones, P. 1999 Representing twentieth-century space-time climate variability. Part I: development of a 1961–90 mean monthly terrestrial climatology. *J. Climate* **12**, 829–856.
- New, M., Hulme, M. & Jones, P. 2000 Representing twentieth-century space-time climate variability. Part II: development of 1901–96 monthly grids of terrestrial surface climate. *J. Climate* **13**, 2217–2238.
- Noble, I. R., Apps, M., Houghton, R. A., Lashof, D., Makundi, W., Murdiyarso, D., Murray, B., Sombroek, W. & Valentini, R. 2000 *IPCC special report on land use, land-use change and forestry*, chapter 2. Cambridge University Press.
- Phillips, O. L. (and 10 others) 1998 Changes in the carbon balance of tropical forests: evidence from long-term plots. *Science* **282**, 439–442.
- Prentice, I. C., Cramer, W., Harrison, S. P., Leemans, R., Monserud, R. & Solomon, A. M. 1992 A global biome model based on plant physiology and dominance, soil properties and climate. *J. Biogeogr.* **19**, 117–134.
- Prentice, I. C., Farquhar, G. D., Fasham, M. J. R., Goulden, M. L., Heimann, M., Jaramillo, V. J., Kheshgi, H. S., Quéré, C. L., Scholes, R. J. & Wallace, D. W. R. 2001 *The carbon cycle and atmospheric carbon dioxide*, chapter 3. Cambridge University Press.
- Proctor, J. 1999 NPP tropical forest: Gunung Mulu, Malaysia, 1977–1978. Dataset, available online at <http://www.daac.ornl.gov>.
- Richey, J. E., Melack, J. M., Aufdenkampe, A. K., Ballester, V. M. & Hess, L. L. 2002 Outgassing from Amazonian rivers and wetlands as a large tropical source of atmospheric CO₂. *Nature* **416**, 617–620.
- Sitch, S. (and 11 others) 2003 Evaluation of ecosystem dynamics, plant geography and terrestrial carbon cycling in the LPJ dynamic global vegetation model. *Global Change Biol.* **9**, 161–185.

- Thonicke, K., Venevsky, S., Sitch, S. & Cramer, W. 2001 The role of fire disturbance for global vegetation dynamics: coupling fire into a dynamic global vegetation model. *Global Ecol. Biogeogr.* **10**, 661–677.
- Tian, H., Melillo, J. M., Kicklighter, D. W., McGuire, A. D., Helfrich III, J. V. K., Moore III, B. & Vörösmarty, C. J. 1998 Effect of interannual climate variability on carbon storage in Amazonian ecosystems. *Nature* **396**, 664–667.
- Uhl, C. & Kauffman, J. B. 1990 Deforestation, fire susceptibility, and potential tree responses to fire in the eastern Amazon. *Ecology* **71**, 437–449.
- Uhl, C., Kauffman, J. B. & Cummings, D. L. 1988 Fire in the Venezuelan Amazon 2: environmental conditions necessary for forest fires in the evergreen rainforest of Venezuela. *Oikos* **53**, 176–184.
- Zobler, L. 1986 A world soil file for global climate modelling. NASA technical memorandum 87802, NASA.

GLOSSARY

- CRU: Climate Research Unit
DGVM: dynamic global vegetation model
GPP: gross primary production
LPJ: Lund–Potsdam–Jena model
NEP: net ecosystem productivity
NPP: net primary productivity
PFT: plant functional type